Characteristics of Raindrop Size Distribution observed in Southern China in different weather scenarios using 2-D video disdrometer

JIN Jeffrey Tong, CHAN Ying-wa
Hong Kong Observatory, Hong Kong, China

Abstract

The characteristics of raindrop size distribution (DSD) in different weather scenarios have been studied using measurements from two-dimensional video disdrometer (2DVD) installed at Chek Lap Kok (CLK) in Hong Kong (HK). Preliminary analysis showed that the mass-weighted mean diameter (D_m) for stratiform (stra.) precipitation (ppt.) fell largely in the range of 0.5 – 2 mm. For convective (conv.) ppt., D_m varied mostly from 1 to 3 mm. Based on the scatterplot of D_m and rainfall rate (R), for conv. precipitation with high R values (> 100 mm/hr), D_m seemed to have plateaued around 2.3 mm. Further increase of R was mainly due to the increase in concentration of raindrops (N_t). The results were consistent with the findings of Wen et al. (2016) for DSD observed in East China.

Instrument and Data

A 2DVD disdrometer operates by using two orthogonal horizontal light sheets that form an effective area for sensing the falling of raindrops. As raindrops fall through the light sheets, they cast a shadow that is recorded by the line-scan cameras for deriving the drop sizes, shapes and other parameters (Fig. 1a). The 2DVD disdrometer installed at CLK in HK in shown in Fig. 1b.

DSD measurements by 2DVD disdrometers in 15 different rainfall events comprising both conv. and strat. ppt. types with some occurred during the influence of tropical cyclones (TC) were analysed. With two sets of 2DVD disdrometers installed at Yang Chun and En Ping over southern China respectively (Fig. 2), comparison was made to analyse the spatial difference of DSDs during the influence of TC Wipha in 2019. Radar echoes showing the typical stra., conv. ppt. types and the outer rainbands of Wipha are shown in Fig. 3a, 3b and 3c respectively.

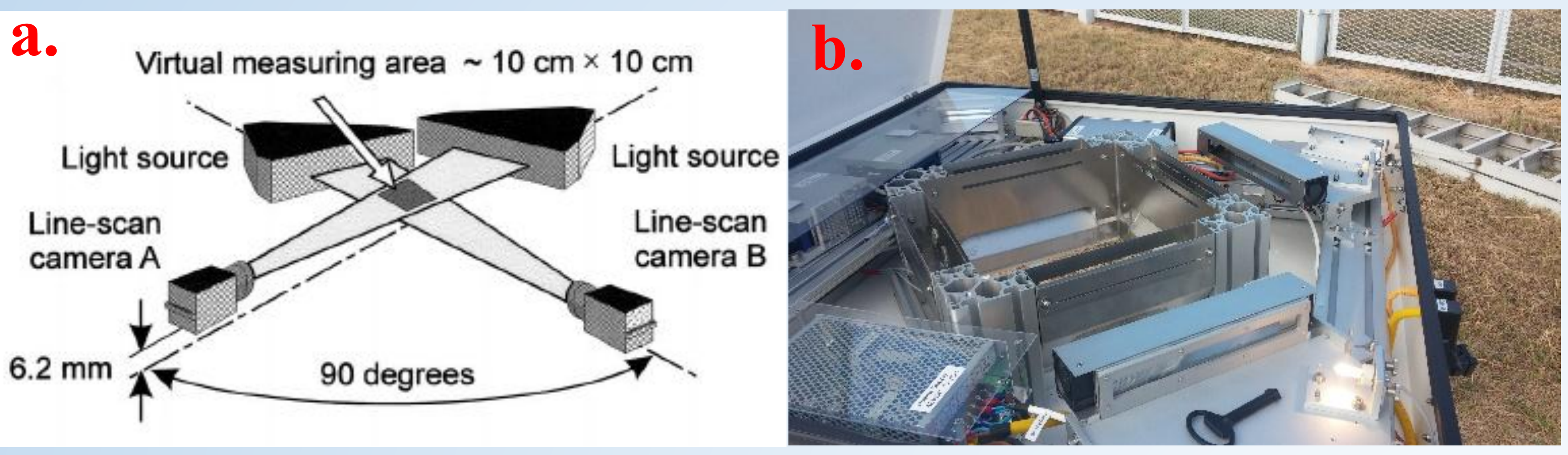

Fig. 1: (a) Operational principle and (b) Photo of the 2DVD at CLK in HK

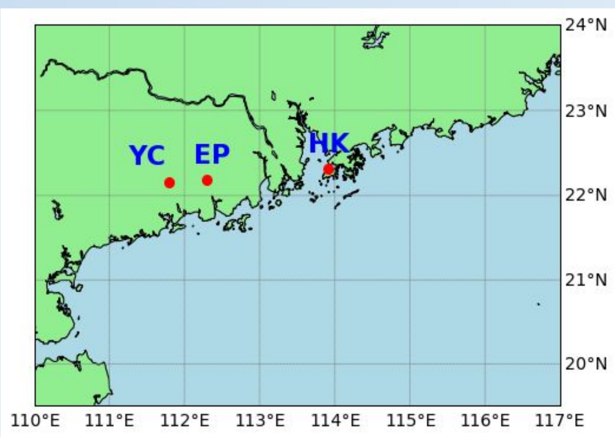

Fig. 2: Locations of the three different sites installed with 2DVD disdrometers at HK, YC and EC respectively over the south China coastal region.

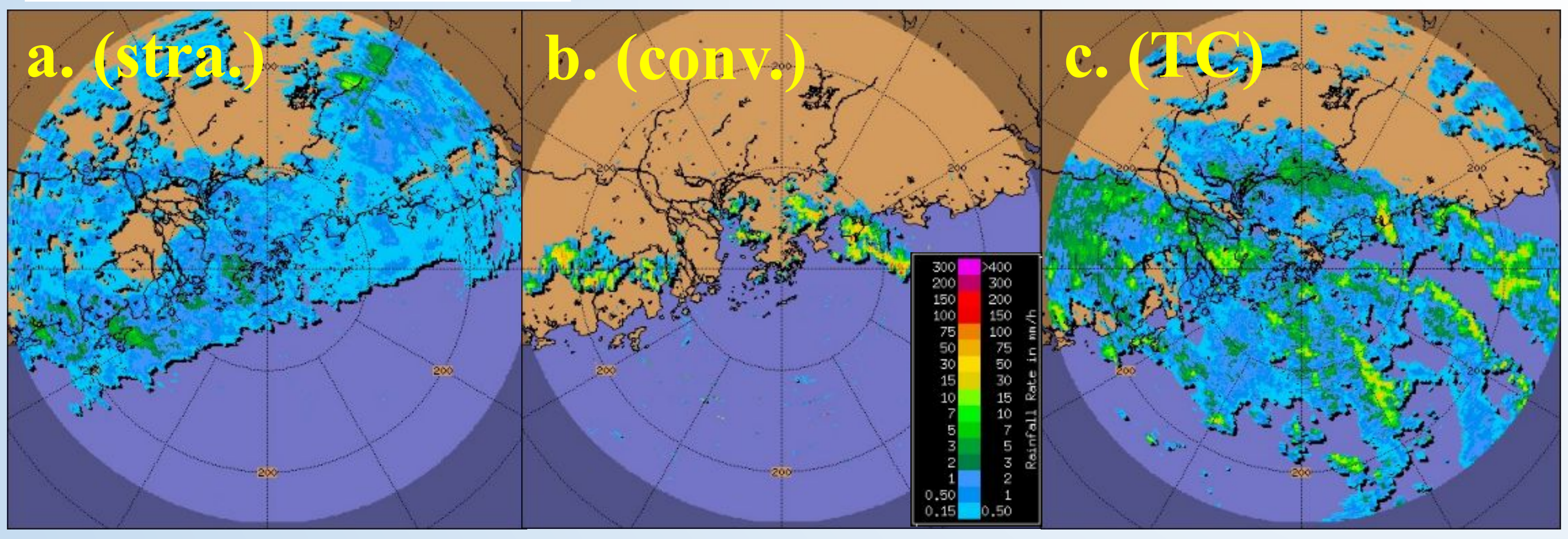

Fig. 3: 3 km CAPPI radar reflectivity images for (a) stra. rainfall at 02:00 UTC on 20 Feb 2022, (b) conv. rainfall at 14:54 UTC on 24 Jul 2021, (b) Rainfall associated with the outer rainbands of TC Wipha at 02:00 UTC on 1 Aug 2019.

Methodology

- 70 raindrop diameter classes, each class with 0.1 mm bin width, spanning from 0.1-0.2 mm, 0.2-0.3mm …… up to 6.9-7.0 mm are devised;
- Physical parameters based on DSD samples collected in 1-minute interval are derived. These include:
  - $N(D_i) = \frac{1}{\Delta t \cdot \Delta D} \cdot \sum_{j=1}^{70} \frac{n_{ij}}{A_j \cdot v_j}$ (Number concentration of raindrops of diameter i in $m^{-3}mm^{-1}$)
  - $N_t = \sum_{i=1}^{70} N(D_i)\Delta D_i$ (Total concentration of raindrops in m^{-3})
  - $R = \frac{6\pi}{10^4} \cdot \sum_{i=1}^{70} {D_i}^3 V_i N(D_i)\Delta D_i$ (Mean rainfall rate in $mmhr^{-1}$)
  - $D_m = \frac{\sum_{i=1}^{70} N(D_i){D_i}^4 \Delta D_i}{\sum_{i=1}^{70} N(D_i){D_i}^3 \Delta D_i}$ (Mass-Weighted Mean Diameter of raindrops in mm)
- Classification of ppt. type, for at least 10 consecutive 1 minute DSD samples:
  - Stra.: R > 0.5 mmh^{-1}, σ_R (standard deviation) < 1.5 mmh^{-1}
  - Conv.: R > 5 mmh^{-1}, σ_R > 1.5 mmh^{-1}

Results and Discussion

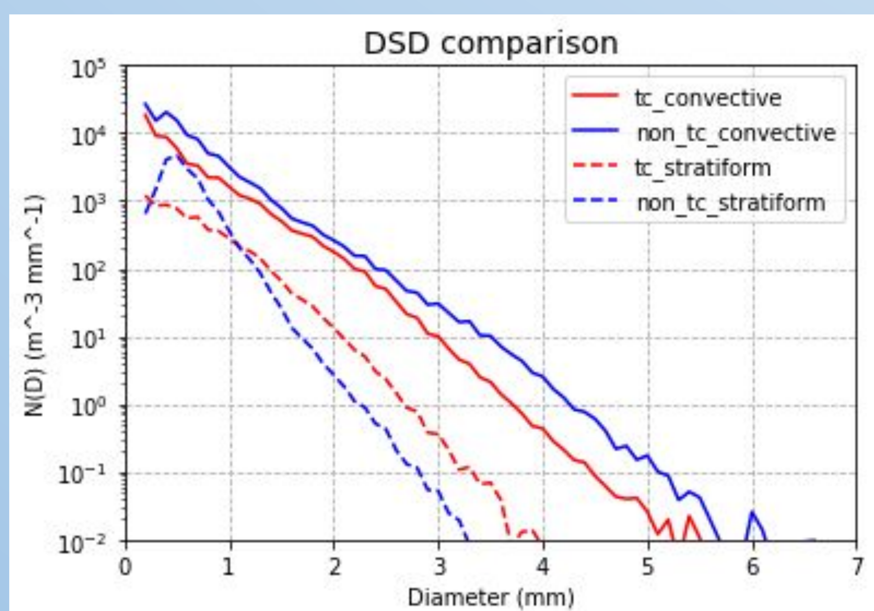

Fig. 4: DSD of conv. (solid lines) and stra. (dashed lines) ppt., under both TC (red lines) and non-TC (blue lines) scenarios recorded in HK.

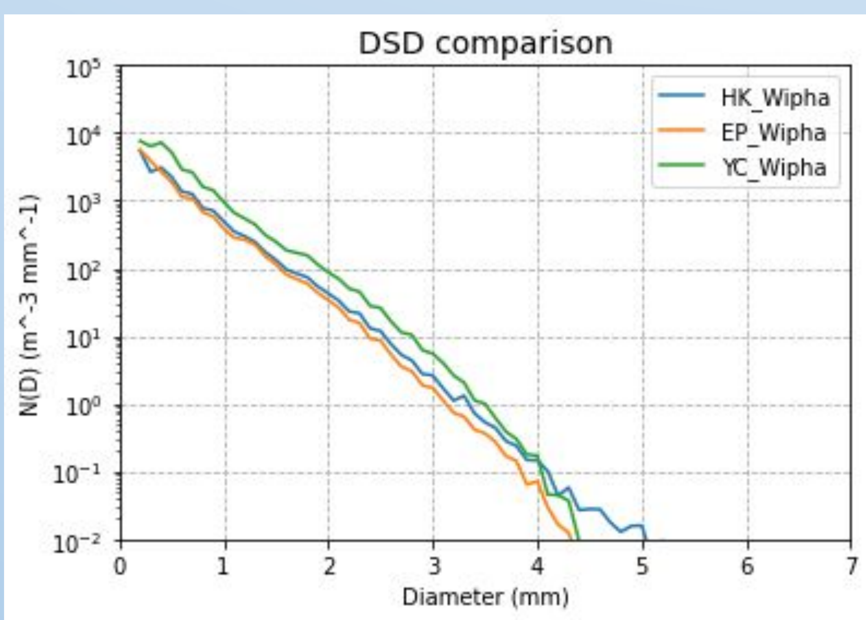

Fig. 5: DSD of ppt. associated with the outer rainbands of TC Wipha (2019) recorded in HK (blue), EP (orange) and YC (green) on 1 August 2019.

1. DSD as represented by $N(D_i)$ *(Fig. 4)*
   - Concentration of raindrops was higher for conv. ppt. (> 10^4 $m^{-3}mm^{-1}$) with the presence of large drops (diameter ≥ 5 mm);
2. DSD associated with the outer rainbands of TC Wipha was similar across the three disdrometer sites at HK, EP and YC respectively. No significant spatial difference was observed *(Fig. 5);*
3. D_m vs. R *(Fig. 6a, b)*
   - Conv. ppt. produced larger raindrops with mean diameter (D_m) >2 mm for R > 100mm/hr. For stra. ppt., D_m was mostly <2 mm; *(Fig. 6a, b);*
   - The increases of D_m with R generally followed a power function. However, for conv. ppt., it was plateaued near 2.3 mm for R >100 mm/hr *(Fig. 6a). For stra. ppt., it was plateaued below 2 mm for R > 10 mm/hr (Fig. 6b);*
4. N_t vs. R *(Fig. 6c, 6d)*
   - For conv. ppt., N_t seemed to be the primary factor causing the increase of R and N_t grew almost linearly as R increased *(Fig. 6c). For* stra. ppt., the general linear increase between N_t and R was observed only in TC scenarios *(Fig. 6d);*
5. TC vs non-TC scenarios *(Fig. 4, 6a-d)*
   - For conv. ppt., D_m was slightly larger in non-TC scenarios *(Fig. 6a);*
   - For stra. ppt., smaller N_t and larger D_m were observed in TC scenarios *(Fig. 6b, d)*
   - Under TC scenarios, the differences in DSD, D_m and N_t between conv. and stra. ppt. were less compared with those under non-TC scenarios *(Fig. 4, 6a-d).*

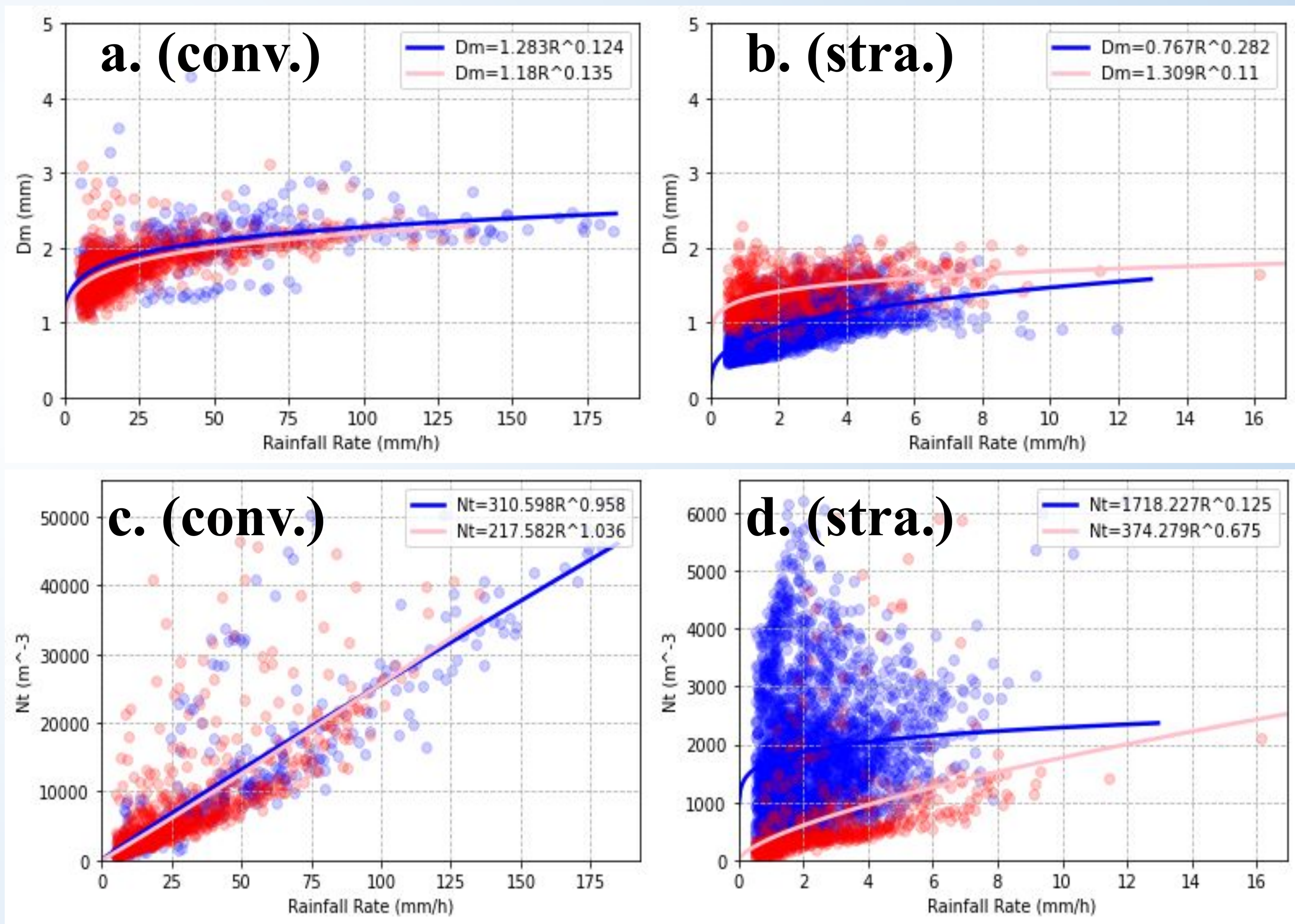

Fig. 6: Scatterplots of D_m vs R (a: conv., b: stra.); N_t vs R (c: conv., d: stra.); blue: non-TC scenarios, red: TC scenarios. The power-fitted curves (solid lines) and equations are also shown.

Summary and Conclusion

1) For conv. ppt, the sizes of raindrops grow by coalescence which leads to the build-up of larger drops. The growth is more effective when the updraft is strong. However, for very high value of R, the rate of coalescence is offset by the rate of breakup so that the increase of D_m is plateaued. Higher R is therefore mainly attributed to the increase of N_t.

2) For stra. ppt., the updraft is weak. The sizes of raindrops grow by deposition, accretion and riming. Given the same R, D_m is smaller but N_t is larger when compared to conv. ppt., particularly in non-TC scenarios.

3) For ppt. associated with the rainbands of TCs, DSDs seem to be quite similar. Under TC scenarios, the differences in DSD, D_m and N_t between conv. and stra. ppt. types are less compared with those in non-TC scenarios. There are also fewer large drops (≥ 5 mm) in conv. ppt., possibly due to weaker updrafts.

References

Bringi, V. N., V. Chandrasekar, J. Hubbert, E. Gorgucci, W. L. Randeu, and M. Schoenhuber, 2003: Raindrop size distribution in different climatic regimes from disdrometer and dual-polarized radar analysis. *Journal of the Atmospheric Sciences*, **60**, 354–365, doi:10.1175/1520-0469(2003)060<0354:rsdidc>2.0.co;2.

Chen, B., J. Yang, and J. Pu, 2013: Statistical characteristics of raindrop size distribution in the Meiyu season observed in eastern China. *Journal of the Meteorological Society of Japan. Ser. II*, **91**, 215–227, doi:10.2151/jmsj.2013-208.

Deo, A., and K. J. E. Walsh, 2016: Contrasting tropical cyclone and non-tropical cyclone related rainfall drop size distribution at Darwin, Australia. *Atmospheric Research*, **181**, 81–94, doi:10.1016/j.atmosres.2016.06.015.

Huang, C., S. Chen, A. Zhang, and Y. Pang, 2021: Statistical characteristics of raindrop size distribution in monsoon season over South China Sea. *Remote Sensing*, **13**, 2878, doi:10.3390/rs13152878.

Kruger, A., and W. F. Krajewski, 2002: Two-dimensional video disdrometer: A description. *Journal of Atmospheric and Oceanic Technology*, **19**, 602–617, doi:10.1175/1520-0426(2002)019<0602:tdvdad>2.0.co;2.

Tokay, A., P. G. Bashor, E. Habib, and T. Kasparis, 2008: Raindrop size distribution measurements in tropical cyclones. *Monthly Weather Review*, **136**, 1669–1685, doi:10.1175/2007mwr2122.1.

Wen, L., K. Zhao, G. Zhang, M. Xue, B. Zhou, S. Liu, and X. Chen, 2016: Statistical characteristics of raindrop size distributions observed in East China during the Asian Summer Monsoon season using 2-D Video disdrometer and Micro Rain Radar Data. *Journal of Geophysical Research: Atmospheres*, **121**, 2265–2282, doi:10.1002/2015jd024160.